

HETEROCYCLES, Vol. 67, No. 2, 2006, pp. 823 - 837. © The Japan Institute of Heterocyclic Chemistry
Received, 28th June, 2005, Accepted, 29th September, 2005, Published online, 30th September, 2005. REV-05-SR(T)2

PHOSPHATE MIMIC OF NUCLEOTIDES, CONFORMATIONAL INFLUENCES ON THE RIBOFURANOSE CONFORMATIONS

Arnaud Gautier

UMR CNRS 6014, IRCOF, Rue Tesnières, F-76821 Mont-Saint-Aignan, France
(On leave to UMR CNRS 6504, Université Blaise Pascal, 24 avenue des Landais, 63177 Aubière CEDEX, France)

Abstract – The influences of the modifications of the natural nucleotides is rationalized in terms of stereoelectronics effects. This article reviews the pseudorotation concept and the Generalized Karplus Type equation used to quantify the conformational behavior of ribofuranose in solution.

Why nature selects phosphate?

Phosphate esters and anhydrides are of paramount importance in the living world. The majority of coenzymes are esters and pyrophosphoric acids, the biochemical energy is stored into phosphorylated compounds such as ATP, the intracellular calcium level is regulated by the action of several inositol phosphates mono and diesters, the genetic material (DNA and RNA) is composed by phosphate diester linkages, the activity of protein is sometimes controlled by phosphorylation processes.

Davis tentatively answered the reason why nature selects phosphate among other functional groups more than 50 years ago.¹ The proposed idea was that organisms must keep their metabolites within the cell and select charged molecules to prohibit passive diffusion through the membranes. The ionized state of the phosphates functions at physiological pH will out a phosphorylated molecule of diffusion.

It is noteworthy that phosphate owns 3 pKa values spreading on all the pH range accessible in water. The Davis principal of “being ionized” is encountered in several biosynthesis where phosphates are implicated in the first step.

Another advantage is the ability of the phosphate to connect two molecular subunit, still being negatively charged (that could not be the case of ester or amide for example).² Weistheimer point another benefit of being ionized: the rate of hydrolysis of phosphates esters is considerably reduced by the electrostatic repulsion between the phosphate and the OH⁻ charges.³ As nature stores genetic material for a long period

of time, the hydrolysis should be minimal at physiological pH. Taking into account that DNA material contains several thousands of phosphate esters bonds per gene, it becomes obvious that a minimum of them should be cleaved during the lifetime of a cell. At biological pH, the negative charge on the phosphate considerably slow down the rate of hydrolysis by a factor of 10^5 - 10^6 .

Why chemists cannot use phosphate for antisense and antigene strategies?

Introduction of small synthetic RNA and DNA in order to intercept natural complementary is the corner-stone of the antisense and antigene strategies. Unfortunately, this is not applicable because of the presence of enzymes that bend and cleave oligonucleotides. Thus, structural modifications of the nucleotides are necessary to increase the half-life of the synthetic partner.⁴ A large numbers of modifications have been proposed and can be classified into 3 parts: the base modification, the phosphate modification and the sugar modification. The first antisense oligomers, active against the Cytomegalovirus introduced on the market, VitraveneTM (ISIS-2922) consist in a 21-mers modified by a phosphorothioate linkage.⁵

Considering that the primary action of enzymes consists in cleaving the linkage at the level of the phosphorus atom, a therapeutic active oligonucleotide should contain stable linkage and should be able to form stable associations.

What make duplexes stable?

Considerable efforts in an attempt to elucidate and quantify the factors responsible for the stability of a double stranded structure have been invested since the 70's. The understanding of the process was greatly facilitated by the adaptation of the principle of pseudorotation. Originally proposed by Kilpatrick in his discussion of the indefiniteness of cyclopentane conformations, Altona and Sundaralingam adapted the principal to the un-symmetric rings such as ribofurranoses, prolines and nucleotides.^{6,7} Their description is useful due to the utilization of the torsion angles that render the Altona-Sundaralingam formalism (referred as the AS formalism) directly usable to NMR spectroscopy.

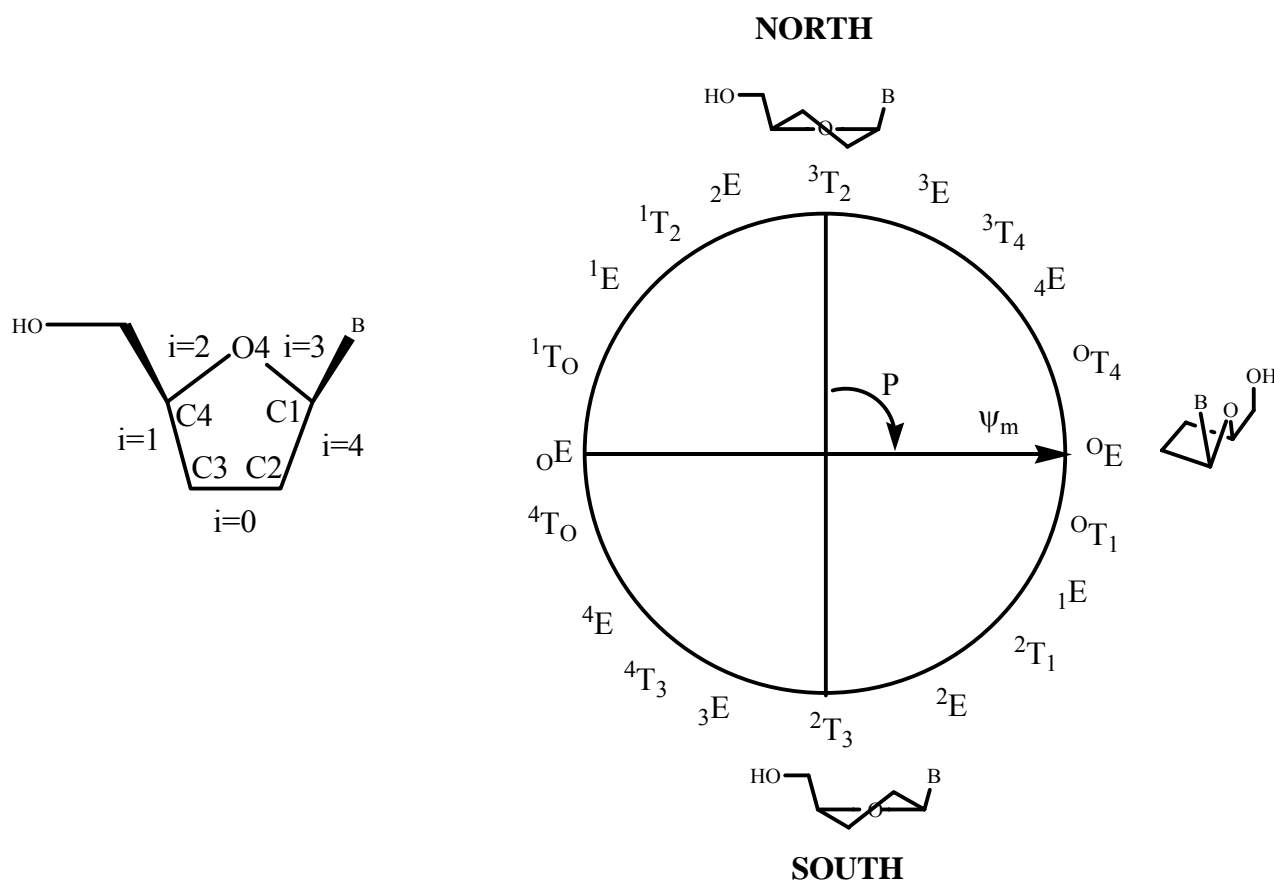
Because of the interrelationship between the endocyclic torsion angles in non-planar 5 membered rings, a quantitative description of puckering and conformation in terms of the maximal puckering angle (ψ_m) and of the phase angle (P) of pseudo-rotation was introduced. The phase angle describes in an exact and mathematical manner the conformation of a given 5 membered ring as a continuum of forms where the standard conformations twists and envelops are located. The maximal puckering angle represents the

maximal deviation from planarity. The central formula used to describe the pseudorotation coordinates is usually referred as the Altona-Sundaralingam equation:

$$\Phi_i = \psi_m * \cos (P + 4\pi i/5) \quad \text{Eq.1}$$

Where Φ_i represents the i^{th} internal torsion angle along the 5-membered ring as define in Figure 1 (according to Altona and Sundaralingam, the C1-C2-C3-C4 torsion angle is chosen as reference, $i=0$).

Figure 1. The pseudorotation wheel representation of nucleotides.



As it can be seen in Eq.1, ψ_m represent the maximum amplitude that an internal torsion angle, Φ_i can adopt. For each Φ_i , this occurs only twice along the pseudo-rotation pathway: when the cosine factor $(P + 4\pi i/5)$ reaches the values 0 and π .

If one disposes of the internal torsion angles, for example from crystallographic data, the puckering coordinates can be deduces from Eqs. 2 and 3:

$$\psi_m = \Phi_0 / \cos(P) \quad \text{Eq. 2}$$

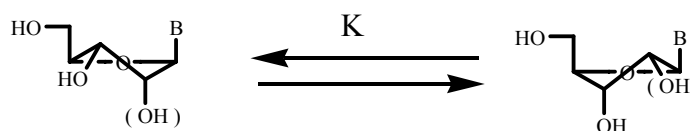
$$P = \arctan [(\Phi_2 - \Phi_1 + \Phi_4 - \Phi_3) / (3.078 \Phi_0)] \quad \text{Eq. 3}$$

With the aid of a crystallographic dataset of 178 X-Rays structures, a statistic survey has shown that the pseudorotation coordinates of nucleotides are presents only in two main regions.⁸ With the aid of the

wheel representation, they were designed as North (N) and South (S) positions (Figure 1). This statistic survey shows that ribonucleic acids are located in the N region, $0^\circ < P^N < 36^\circ$ and in the S region $144^\circ < P^S < 180^\circ$ within an average ψ_{\max} of 38° for the both; regarding the deoxyribonucleic acids, the same tendency is observed with a minor ψ_{\max} averaged at 36° .

The studies of the nucleotides and nucleosides in solution have revealed the same tendency. Every nucleic acid is in equilibrium between a N and a S form, the equilibrium constant being roughly 50%. Therefore, a good representation of a nucleic acid in solution consists in a vector of 5 dimensional hyperspace: $(P^N, \psi_{\max}^N, P^S, \psi_{\max}^S, K)$.

Figure 2. Two state model of pseudorotamers in solution.



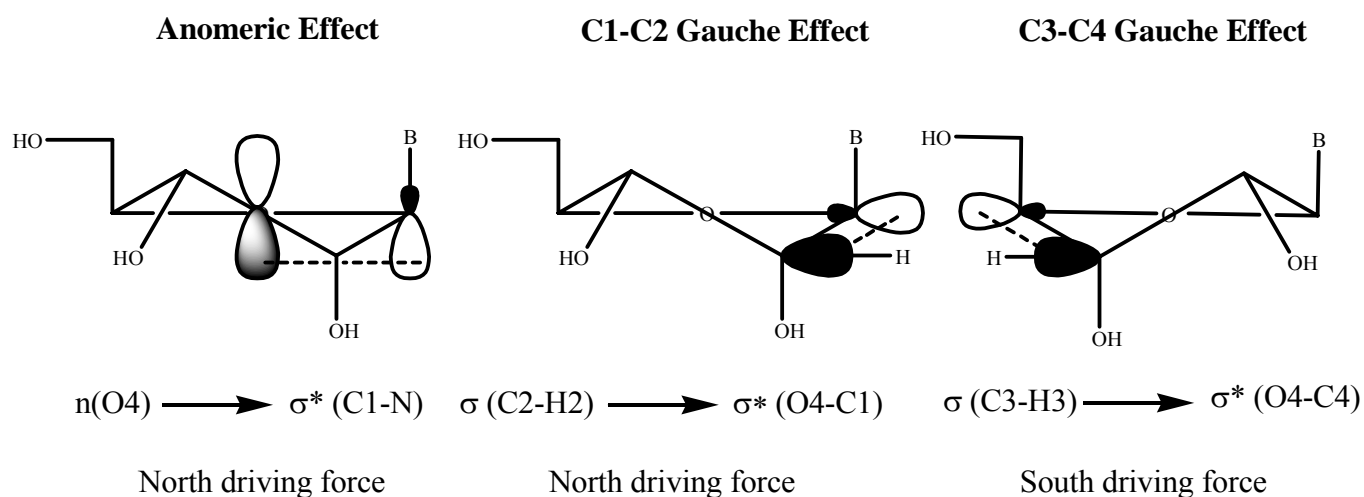
The activation energy barrier for the interconversion between the two preferred puckering modes (North and South) is small, $\Delta G^\ddagger = 20$ to 25 kJ/Mol.⁹ The result of this small barrier is an averaging of the NMR picture, neither a pure N nor a pure S pseudorotamer is spectroscopically visible but only the averaged spectrum is detectable.¹⁰

In a double stranded structure, RNA usually forms A type duplex characterized by an N type conformation of the nucleic acids in both parts of the helix, DNA forms usually B (S type) and in a less extend A (N type) type duplex. Because the association of two strains into a double-strained structure proceeds via a negative variation of entropy ($\Delta S < 0$), this association is entropically unfavorable ($\Delta G = \Delta H - T\Delta S$) and it is better to pre-organize the synthetic strains close to the conformation present in the helix. The BNA (Bridge Nucleic Acid) and LNA (Locked Nucleic Acid) structures independently introduced by Imanishi and Wengel is a typical example of the pre-organization principle.

Chattopadhyaya and al. have lighted the factors governing the conformational behavior of a given nucleotide quite recently.⁹ From a large number of thermodynamic studies and with the aid of the Pseurot Program,¹¹ they showed that the $N \rightleftharpoons S$ equilibrium is the result of a fine balance between anomeric (AE) and gauche effects (GE) of the different substituents present on the ring. The AE and GE are interactions between donor and acceptor orbitals, the stabilisation is directly proportional to the square of the overlap between the two orbitals and inversely proportional to their energy difference.^{9,12} The AE represents the overlapping stabilization by a lone pair of O4(donor) and the anti bonding orbital C1-Base (acceptor). This effect is base and pH dependant but invariably drive the $N \rightleftharpoons S$ equilibrium toward a N position.¹³ In the case of the GE, the donor is a $\sigma(C-H)$ and the acceptor is the $\sigma^*(O4-C)$. The GE is

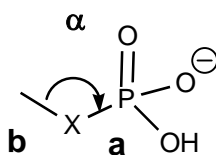
maximal with strongly electronegative substituents and decrease with the electronegativity.¹³ A consequence is depicted by the C2-deoxyribose series in which the electronegativity of the C3 substituent dictates the N \rightleftharpoons S equilibrium.¹⁵ With strong electronegative substituents at the C3 position, the S conformation dominates (91% in case of F). Decreasing the electronegativity at the C3 substituent makes the AE preponderant and result in a shift of the N \rightleftharpoons S equilibrium to a N conformation (75% in the case of NH₂). A global thermodynamic model accounting for the different AE and GE have been proposed and represent relatively well the observations.^{13b}

Figure 3: Stereoelectronic effects in nucleotides



Considering the experimental proofs of the stereoelectronic model we embark in the synthesis of nucleotides devoted to the antisense strategy possessing a hydrolytically stable junction at the C3 position and a low electronegativity.

Table 1: Bond angles, lengths and pKa of the phosphate function and several of its mimics.



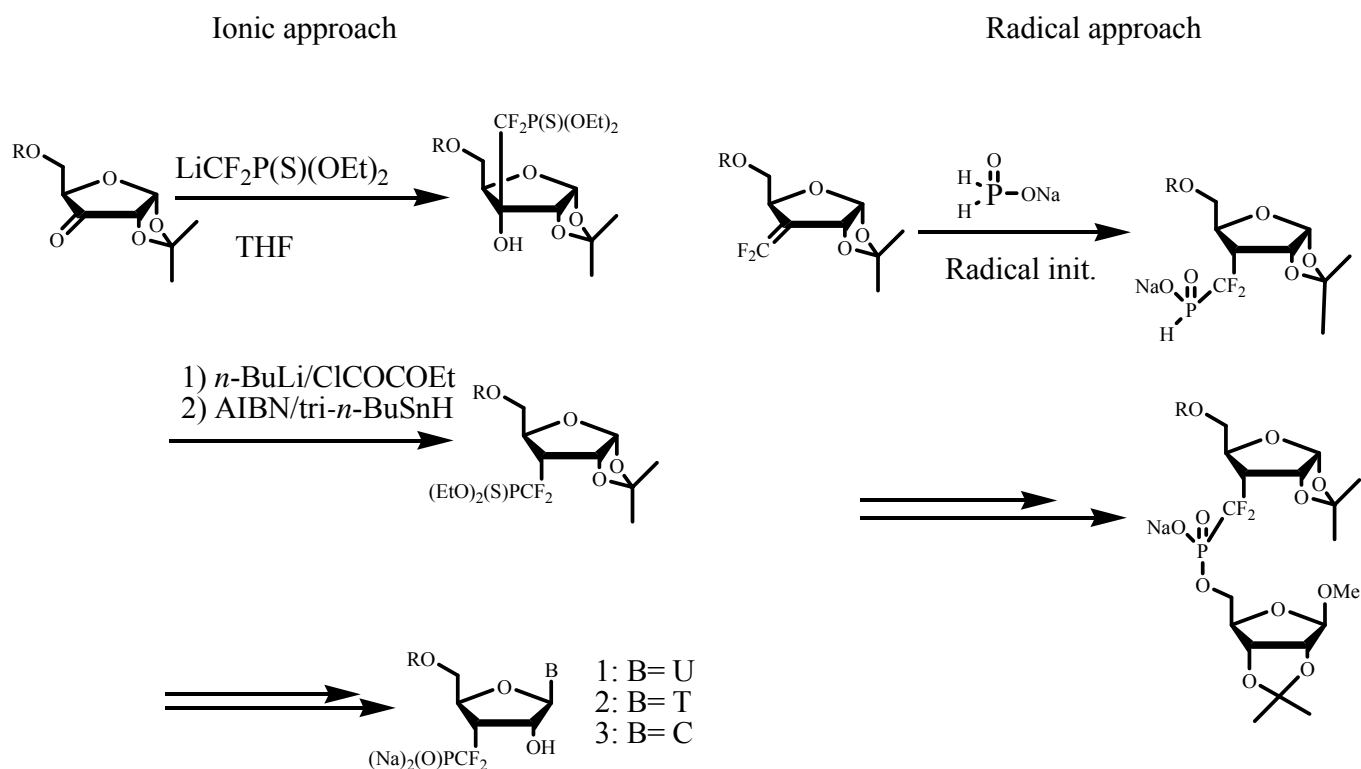
X	α	a	b	pKa ₂
O	118.7°	1.59 Å	1.43 Å	6.4
CH ₂	112.1°	1.81 Å	1.51 Å	7.5
CHF	113.3°	1.82 Å	1.50 Å	6.5
CF ₂	116.5°	1.85 Å	1.50 Å	5.6

Our choice was attracted to the phosphonate family because of the lower Pauling electronegativity of the carbon atom. In the phosphonate series, presently considered as best mimic of the phosphate function, are the monofluorophosphonates (MFP) and the difluorophosphonates (DFP) in which the hydrolysable P-O bond is replaced by a stable P-CHF and P-CF₂ bond respectively.¹⁶⁻¹⁸ Our final choice was then directed to the DFP group in which stereo-complication cannot arise.

Ionic and radical synthesis of C3-DFP modified nucleoside¹⁹

The synthesis of C3 modified nucleotides have been previously reported.^{19e} It can be achieved by an anionic addition onto the properly substituted ketone or by a radical addition of hypophosphorous acid salt onto a gem difluoro olefin. The general scheme is reported below.

Scheme 1. Synthesis of C3 modified nucleoside.



The DFP mimic dictates the conformational behavior of the ribose; a question about mimics.²⁰

As mentioned previously, the N \rightleftharpoons S equilibrium is a function of the balance between the anomeric effect (AE) and several gauche effects (GE) in which the group electronegativity is playing a fundamental role. Thus, one could expect that a CF₂PO₃²⁻ group, aside from its steric difference with the phosphate, can influence the conformational behavior by its intrinsic electronegativity.

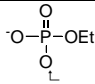
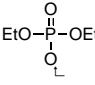
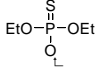
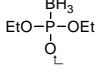
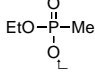
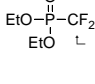
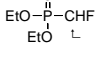
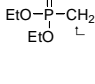
Among all the electronegativity scales available, the one proposed by Inamoto (ι : iota factor) shows one of the best correlations between the enthalpy of the $N \rightleftharpoons S$ equilibrium in nucleotides and the group electronegativity.¹⁵ Another advantage of the Inamoto's scale is a linear relation between the ι factor and the ^{13}C chemical shift of methylene carbon in ethane fragments $\text{CH}_3\text{-CH}_2\text{-X}$ (where X is the considered group).²¹ Thus, a simple experiment can quantify the group electronegativity according to Inamoto's relation:

$$\delta = 59.4 (\iota - 2) + 7.77 \quad \text{Eq. 4}$$

(Correlation factor $r = 0.96$)

In Inamoto's scale the atomic ι factor ranges from 2.0 for hydrogen to 3.1 for fluorine.

Table 2. Electronegativity (ι factor) of phosphate diester and several phosphate mimics.²⁰

Entry	Compound	Group ^(a)	δ (ppm)	ι factor
1	$(\text{Et}_3\text{NH}, \text{O})(\text{EtO})_2\text{P}(\text{O})$		65.9	2.97
2	$(\text{EtO})_3\text{P}(\text{O})$		64.1	2.95
3	$(\text{EtO})_3\text{P}(\text{S})$		64.0	2.95
4	$(\text{EtO})_3\text{P-BH}_3$		62.4	2.92
5	Group I $(\text{EtO})_2\text{P}(\text{O})\text{Me}$		61.0	2.86
6		Group II $(\text{EtO})_2\text{P}(\text{O})\text{N}(\text{Et})_2$		
7	$(\text{EtO})_2\text{P}(\text{O})\text{CF}_2\text{Et}$		27.3	2.33
8	$(\text{EtO})_3\text{P}(\text{O})\text{CFHEt}$		23.1	2.26
9	Group III $(\text{EtO})_2\text{P}(\text{O})\text{CH}_2\text{Et}$		15.9	2.14

(a): the arrows represent the point of substitution.

It becomes clear that not all the considered phosphates analogues belong to the same electronegativity domain.

The group I contains analogues of electronegativity similar to phosphate. Thus, thio phosphonate, phosphonoboronate and methyl phosphonate could be classified as close electronegative mimics.

Group II contains one example of the phosphoramidate function, a widely used analogue since Gryaznov's disclosure.²² The introduction of the nitrogen atom places the ι value at a borderline position in the Inamoto's scale. This electronegativity fall is one of the physical factors called to explain the higher affinity in the duplex formation with C3 phosphoramidate-modified nucleotides.

The carbon family in entries 7-9 of the group III is representative of DFP, MFP and simple phosphonate groups. As expected, the electronegativity increases with the number of fluorine atoms (from 2.14 to 2.33) but cannot reach high ι values and stays below the electronegativity of a phosphoramidate.

The gauche effect occurs in the case of electronegative substituents supported by ethyl fragments and favors a gauche orientation. When a poorly electronegative substituent (group III) replaces a highly electronegative substituent (group I) one could expect that the gauche effect will vanish or at least decrease. This occurs for compounds (**1**) in which the C3 phosphate function has been replaced by the DFP mimic. We used the Pseurot 6.3 software package to get more information about the $N \rightleftharpoons S$ equilibrium and the exact pseudo-rotation coordinates of compound (**1**).¹¹

Pseurot consist in an iterative, non-linear Newton-Raphson procedure that minimize the difference between calculated and measured ^1H - ^1H (or ^1H - ^{19}F in the last version) coupling constants using an error function, the Root Mean Square (RMS):

$$\text{RMS} = [(1/n) (\text{J}^{\text{meas.}} - \text{J}^{\text{calc.}})^2]^{1/2} = f(\text{P}_1, \psi_1, \text{P}_2, \psi_2, \text{X}) \quad \text{Eq. 5}$$

n is the total number of observed coupling constant.

In a two state model, 5 coordinates per temperature allow to calculate the RMS: (P_N, ψ_N) , (P_S, ψ_S) and the percentage of a given component X , necessary to describe the $N \rightleftharpoons S$ state. Using the Altona-Sundaralingam formula (Eq.1) and a Generalized Karplus type Equation (GKE), it is thus possible to simulate any $^3\text{J}(^1\text{H}-^1\text{H})$ coupling constant and calculate the RMS function. The best fit between measured and calculate $^3\text{J}(^1\text{H}-^1\text{H})$ corresponds to the minimum of the function (but not necessary zero). At the minimum of the RMS function, all the partials derivatives from P_N , ψ_N , P_S , ψ_S and X vanish. The Newton-Raphson method consist in calculating the first derivative (gradient) and the Hessian matrix of the RMS function, solving the system $\text{H}\delta = \nabla$ ($\text{H}_{ij} = \delta^2\text{F}/\delta x_i \delta x_j$ and $\nabla_i = \delta\text{F}/\delta x_i$ are respectively the elements of the Hessian matrix and the elements of the gradient vector of the RMS function, δ represents the variation of the coordinates P , ψ , and X) and re-iterate until the norms of δ or ∇ converge to a very small value.

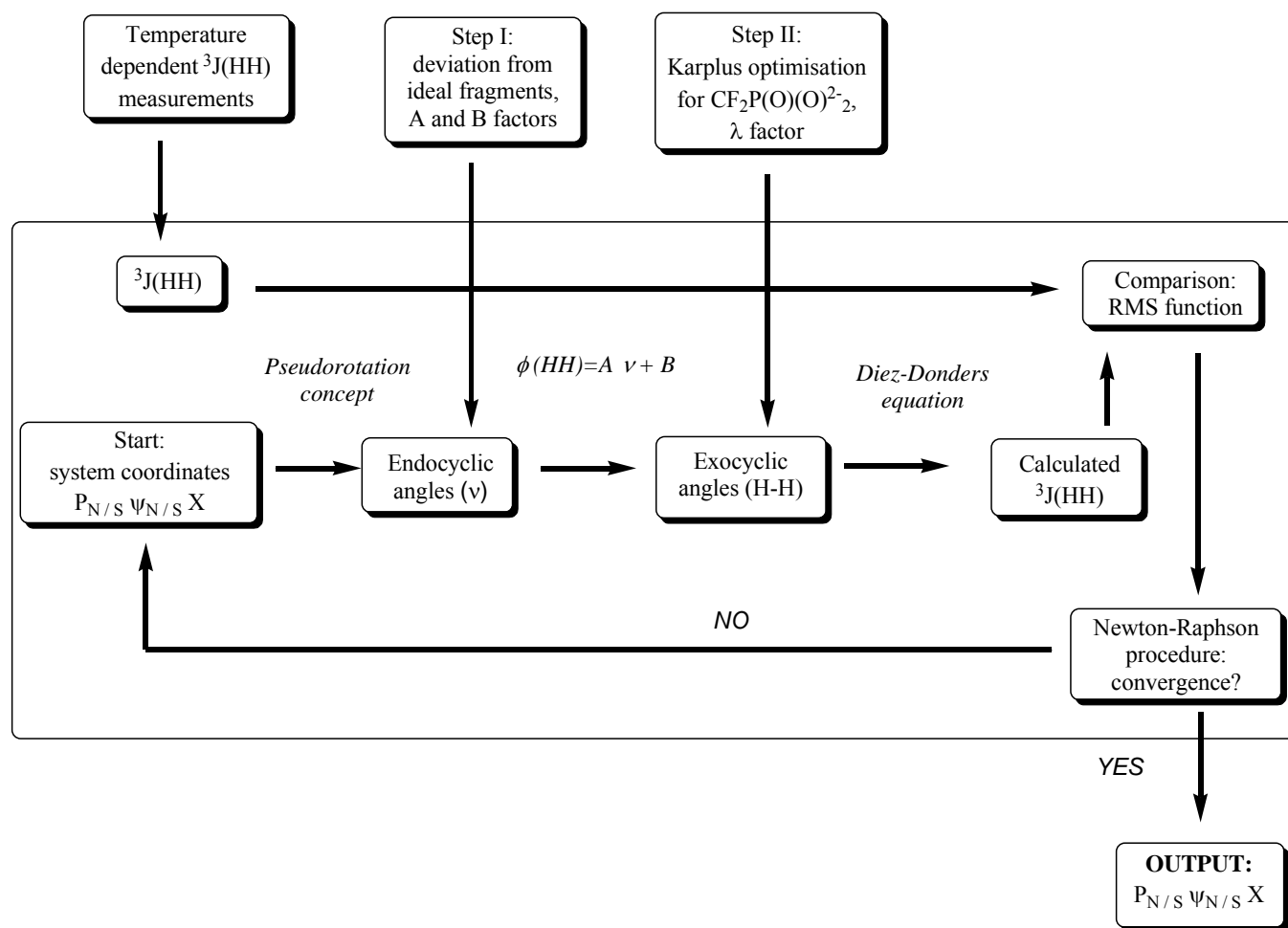
The Figure 4 presents the Pseurot program created by van Wijk, Haasnoot, de Leeuw, Huckriede, Westra Hoekema and Altona at the Leiden Institute of Chemistry. The last update (1999, version 6.3) by Westra

Hoekzema not only use the simple proton-proton coupling data but also offer other possibilities such as the sums of the couplings constants, useful in case of overlapping signals, and a Generalized Karplus Equation designed for proton-fluorine coupling that is of great importance for the analysis of several fluorine modified nucleotides.

Figure 4: The Pseurot procedure

PSEUROT PROGRAM

INPUT:
Experimental measurements
and *ab initio* calculations



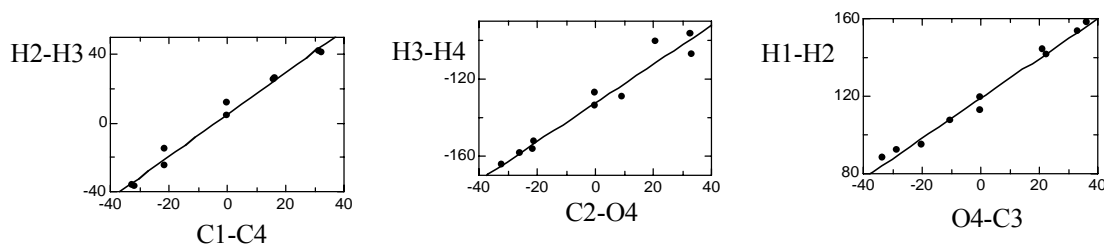
A general problem occurring in the determination of the parameters of pseudorotation of five membered rings is the deviation from the ideal fragments induced by the strain (step I in Figure 4). Thus, the translations between *endo* Φ_e and *exocyclic* $\Phi(HH)$ angles are not represented by $\Phi_e = \Phi(HH) \pm 120$ or 0 but by the relation:

$$\Phi_e = A * \Phi(HH) + B$$

A and B factors encounter for the deviation. These factors are usually determined by a series of *ab initio* calculations.²⁰

The following scheme represents the determination of A and B factors applied to our DFP modified nucleotide.

Figure 5. The plot of the endo vs exocyclic torsion angles of compound (1).



The A and B values corresponding to the 3 angles of interest are collected in table 3:

Table 3. Factors encountering for the deviation from ideal fragments in compound 1.

Torsion angles	A	B	Correlation
O4-C1-C2-C3	1.03	118.8	0.99
C1-C2-C3-C4	1.22	4.9	0.99
C2-C3-C4-O4	1.09	-132.5	0.98

In step II of Figure 4, the KGE used in the Pseurot program is the up-to-date optimized proposed by Diez, Donders and al.²³ This equation considers a coupling constant as periodic function of the torsion angle, meaning that after a rotation of 360°, the value of the coupling constant is found back.

$${}^3J(\alpha) = C_0 + C_1 \cos(\alpha) + C_2 \cos(2\alpha) + C_3 \cos(3\alpha) + S_2 \sin(2\alpha) \quad \text{Eq. 7}$$

The cosine and sinus coefficients depend of the substitution pattern and are calculated by the following set of equations:

$$C_0 = 6.97 - 0.58 (\lambda_1 + \lambda_2 + \lambda_3 + \lambda_4) - 0.24 (\lambda_1 \lambda_2 + \lambda_3 \lambda_4) \quad \text{Eq. 8}$$

$$C_1 = -1.06 \quad \text{Eq. 9}$$

$$C_2 = 6.55 - 0.82 (\lambda_1 + \lambda_2 + \lambda_3 + \lambda_4) + 0.20 (\lambda_1 \lambda_4 + \lambda_2 \lambda_3) \quad \text{Eq. 10}$$

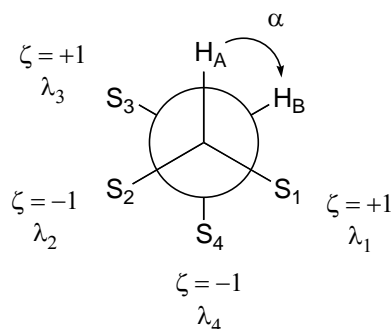
$$C_3 = -0.54 \quad \text{Eq. 11}$$

$$S_2 = 0.68 (\zeta_1 \lambda_1^2 + \zeta_2 \lambda_2^2 + \zeta_3 \lambda_3^2 + \zeta_4 \lambda_4^2) \quad \text{Eq. 12}$$

λ , named "empirical electronegative factor" is an empirical parameter accounting for the influence of the i^{th} substituent to the coupling constant and ζ is an orientation parameter ($\zeta = \pm 1$), its value depending on

the spatial relation of the considered substituent with respect to the geminal coupling proton as depicted in the Figure 6.²⁴

Figure 6. Numbering and sign convention used for an ethane fragment.



The λ parameter corresponding to the difluorophosphate group was determined according to the relation reported by Altona *et al.* in 1994 and specially adapted to a $\text{CH}_3\text{-CHR}_1\text{R}_2$ fragment.²⁵ In this case, the fast rotation of the methyl group causes the cosine and sinus orientation factors to vanish.

$${}^3J = 7.660 - 0.596(\lambda_1 + \lambda_2) - 0.419(\lambda_1 \lambda_2) \quad \text{Eq. 13}$$

In this procedure, λ_1 varies from known group values and λ_2 represents the unknown value of the DFP group. The experimental determination of the λ factor (within an accuracy of ± 0.02 Hz) is depicted in the table 4.

Table 4. Determination of the λ factor.

Subst.	λ_2 value (subst.)	3J obs. (Hz)	Calcd. λ_1	Back calcd. (Hz)	ΔJ ((Hz)
H	0	7.50	0.27	7.51	-0.01
OH	1.25	6.66	0.23	6.64	0.02
OAc	1.17	6.70	0.25	6.69	0.01
Me	0.80	6.95	0.24	6.95	0.00

From the experimental determination, the DFP group holds a λ factor of 0.25. This value differs considerably from the reported value of the phosphate function, 1.27, and it ensues that a computed 3J value from a GKE will diverge between these two groups.

Having optimized both the Diez-Donders's GKE and the deviation from ideal fragments, the Pseurot procedure could be launch using a dataset of ${}^3J(\text{H}^1\text{-H}^1)$ coupling constants collected over a large range of temperatures.

The 7 temperature dependent measurements allow calculating 11 unknown parameters (P_N , ψ_N , P_S , ψ_S and 7 thermodynamics parameters, X) from $7 \times 3 = 21$ physical determinations. The percentage of north conformer and the error analysis is depicted in table 5.

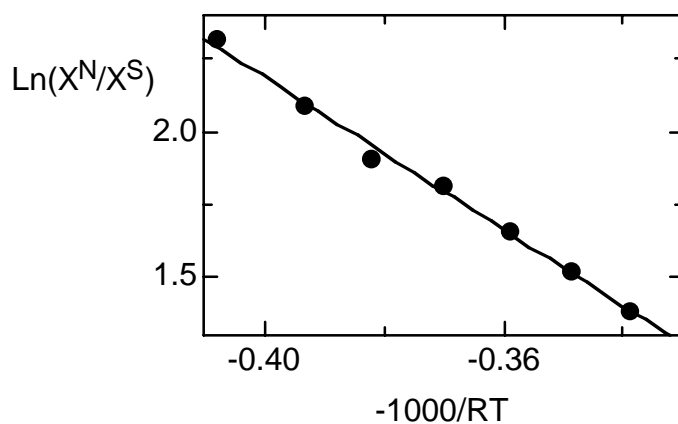
Table 5: ${}^3J_{H,H}$ coupling constants (Hz) ^(a), population and error analysis over 7 temperatures.

T(K)	${}^3J_{1,2'}$	${}^3J_{2,3'}$	${}^3J_{3,4'}$	X(%)	ΔJ_{max} (Hz)	RMS(Hz)
295	1.42	5.32	10.30	98	0.07	0.06
306	1.45	5.45	10.19	95	0.02	0.02
315	1.42	5.54	10.15	95	0.07	0.06
325	1.70	5.61	10.08	90	0.01	0.01
335	1.85	5.72	10.04	87	0.05	0.03
345	1.99	5.79	9.90	83	0.01	0.01
355	2.02	5.85	9.85	82	0.02	0.02

^a the accuracy of the measurement is ± 0.03 Hz

The optimization smoothly converges to a minimum representing a two states equilibrium located at $P_N = 27^\circ$, $\psi_N = 25^\circ$ (a ${}^3E-{}^3T_4$ conformation); $P_S = 105^\circ$, $\psi_S = 24^\circ$ (${}^0E-{}^0T_1$ conformation). As the percentage of the N and S conformers are now accessible at various temperatures, the van't Hoff plot of $\ln(X^N/X^S)$ as a function of $-1000/RT$ delivers the thermodynamics parameters of the equilibrium.

Figure 7. van't Hoff plot $\ln K$ vs $-1000/RT$ for compound **(1)** corresponding to a $S \rightleftharpoons N$ equilibrium.



With a good correlation coefficient of 0.998, the van't Hoff plot reveals an enthalpy contribution of $\Delta H = -13 \text{ kJ} \cdot \text{mol}^{-1}$ and an entropy contribution of $\Delta S = -3 \text{ kJ} \cdot \text{mol}^{-1} \cdot \text{K}^{-1}$. This clearly shows that the enthalpy contribution is the main factor that drives the equilibrium toward the N conformer.

The percentage of the N component is relatively high regarding the situation of the corresponding natural nucleotide: $X_N = 98\%$ at 295K for the C3 DFP modified nucleotide and $X_N = 57\%$ at 278K for the unmodified compound. This high percentage of N conformer is the results of the low electronegativity of the DFP group (t : 2.33 vs. 2.97) that decreases the gauche effect along the C3-C4 bond. The remaining predominant factors are two gauche effects present on the C1-C2 fragments: O4-O2 and the O2-Base gauche effects, the former driving the equilibrium to N and the later smoothly S in the case of Uridine. In addition, the anomeric effect drives the equilibrium to a N position. Qualitatively, the overall contribution would shift the equilibrium strongly to a N position.

The reported study of the conformational behavior of a C3 DFP modified nucleotide questions about the general definition of a mimic. The primary reports concerning DFP groups were focused on the pKa, bond angles and lengths. From crystallographic structures it is clear that MFP and DFP are more close to phosphate than a phosphonate could be. Nevertheless, it is clear that a DFP is not a simple bond length and angle mimic; the influence on the global conformational behavior in solution that is of paramount importance for a duplex stability, should also be taken into account. Considering this matter, not only static data from X-Rays should be considered but also more fine influences.

ACKNOWLEDGEMENTS

A.G. thanks Pr Barry M. TROST for a post-doctoral stage in his laboratory during 1997-1998.

REFERENCES

1. B. D. Davis, *Arch. Biochem. Biophys.*, 1958, **78**, 497.
2. F. H. Westheimer, *Sciences*, 1987, **235**, 1173.
3. J. Kumamoto and F. H. Westheimer, *J. Am. Chem. Soc.*, 1955, **77**, 2515.
4. (a) E. Uhlmann and A. Peyman, *Chem. Rev.*, 1990, **90**, 543; (b) A. H. R. de Mesmaeker, P. Martin, and H. E. Moser, *Acc. Chem. Res.*, 1995, **28**, 366.
5. S. T. Crooke, *Antisense Nucleic Acid Drug Dev.*, 1998, **8**, vii-viii.
6. (a) J. E. Kilpatrick, K. S. Pitzer, and R. Spitzer, *J. Am. Chem. Soc.*, 1947, **69**, 2483; (b) K. S. Pitzer and W. F. Donath, *J. Am. Chem. Soc.*, 1959, **81**, 3213.
7. (a) C. Altona, H. J. Giese, and C. Romers, *Tetrahedron*, 1968, **24**, 13; (b) C. Altona and M. Sundaralingam, *J. Am. Chem. Soc.*, 1972, **94**, 8205; (c) C. Altona and M. Sundaralingam, *J. Am. Chem. Soc.*, 1973, **95**, 2333.
8. H. P. M. de Leeuw, C. A. G. Haasnoot, and C. Altona, *Isr. J. Chem.*, 1980, **20**, 2783.
9. C. Thibaudeau, P. Acharya, and J. Chattopadhyaya, 'Stereolectronics Effects in Nucleosides and

Nucleotides and their Structural Implications', Uppsala University Press, Uppsala, 2002.

10. (a) H. P. M. de Leeuw, J. R. de Jager, H. J. Koeners, J. H. van Boom, and C. Altona, *Eur. J. Biochem.*, 1977, **76**, 209; (b) H. Plach, E. Westhof, H. D. Lüdemann, and R. Mengel, *Eur. J. Biochem.*, 1977, **80**, 295; (c) E. Westhof, H. Plach, I. Cuno, and H. D. Lüdemann, *Nuclei Acids Res.*, 1997, **4**, 939.
11. Pseurot 6.3; Leiden Institute of Chemistry, Leiden University: Leiden, The Netherlands, 1999.
12. (a) E. A. C. Lucken, *J. Chem. Soc.*, 1959, 2954; (b) C. Romers, C. Altona, H. R. Guys, and E. Havinga, *Topics in Stereochemistry*, ed. by E. L. Eliel and N. L. Allinger, Wiley, Intersciences, New York, 1969, p. 39; (c) C. L. Perrin, K. B. Armstrong, and M. A. Fabian, *J. Am. Chem. Soc.*, 1994, **116**, 715.
13. (a) J. Plavec, W. Tong, and J. Chattopadhyaya, *J. Am. Chem. Soc.*, 1993, **115**, 9734; (b) P. Acharya, A. Trifanova, C. Thibaudeau, A. Foldesi, and J. Chattopadhyaya, *Angew. Chem., Int. Ed.*, 1998, **38**, 4645.
14. S. Wolfe, *Acc. Chem. Res.*, 1972, **5**, 102; K. B. Wiberg, *Acc. Chem. Res.*, 1996, **29**, 229.
15. C. Thibaudeau, J. Plavec, N. Garg, A. Papchikhin, and J. Chattopadhyaya, *J. Am. Chem. Soc.*, 1994, **116**, 4038.
16. For phosphonates: (a) D. F. Wiemer, *Tetrahedron*, 1997, **53**, 16609; (b) R. Engel, *Chem. Rev.*, 1977, **77**, 349; (c) H. An, T. Wang, and P. D. Cook, *Tetrahedron Lett.*, 2000, **41**, 7813; (d) H. An, T. Wang, M. A. Maier, M. Manoharan, B. S. Ross, and P. D. Cook, *J. Org. Chem.*, 2001, **66**, 2789.
17. For monofluorophosphonate (MFP): (a) R. D. Chambers, R. Jahouari, and D. O'Hagan, *Tetrahedron*, 1989, **45**, 5101; (b) R. D. Chambers, D. O'Hagan, R. B. Lamont, and S. C. Jain, *J. Chem. Soc., Chem. Comm.*, 1990, 1053; (c) D. B. Berkowitz, M. Bose, T. J. Pfannenstiel, and T. Doukov, *J. Org. Chem.*, 2000, **65**, 4498; (d) D. B. Berkowitz and M. J. Bose, *J. Fluorine Chem.*, 2001, **112**, 13.
18. For difluorophosphonate (DFP): (a) G. M. Blackburn, D. A. England, and F. Kolkman, *J. Chem. Soc., Chem. Comm.*, 1981, 930; (b) C. E. Mc Kenna and P. -D. Shen, *J. Org. Chem.*, 1981, **46**, 4573; (c) G. M. Blackburn, D. E. Kent, and F. Kolkman, *J. Chem. Soc., Chem. Comm.*, 1981, 1188; (d) G. M. Blackburn and D. E. Kent, *J. Chem. Soc., Perkin Trans. 1*, 1986, 913; (e) D. P. Phillion and D. G. Cleary, *J. Org. Chem.*, 1992, **57**, 2763; (f) T. R. Jr. Burke, H. K. Kole, and P. P. Roller, *Biochem. Biophys. Res. Commun.*, 1994, **204**, 129; (g) S. Halazy, A. Ehrhard, A. Eggenpiller, V. Berges-Gross, and C. Danzin, *Tetrahedron*, 1996, **52**, 177; (h) Y. Higashimoto, S. Saito, X. -H. Tong, A. Hong, K. Sakaguchi, E. Appella, and C. W. Anderson, *J. Biol. Chem.*, 2000, **275**, 23199.
19. For ionic approach: (a) L. Lopin, A. Gautier, G. Gouhier, and S. R. Piettre, *J. Am. Chem. Soc.*, 2002, **124**, 14668. (b) I. Kalinina, A. Gautier, C. Salcedo, J.-Y. Valnot, and S. R. Piettre, *Tetrahedron*, 2004, **60**, 4895. For radical approach: (c) A. Gautier, G. Garipova, C. Salcedo, S. Balieu, and S. Piettre, *Angew. Chem., Int. Ed.*, 2004, **43**, 5963. (d) O. Dubert, A. Gautier, E. Condamine, and S. Piettre, *Organic Lett.*, 2002, **4**, 359. The synthesis and the applications have already been reviewed in details: (e) A. Gautier, C. Lopin, G. Garipova, I. Kalinina, C. Salcedo, S. Balieu, and S. Piette, *J. Fluorine*

- Chem.*, 2004, **125**, 1745.
20. C. Fressigné, S. Piettre, E. Condamine, C. Altona, and A. Gautier, *Tetrahedron*, 2005, **61**, 4769.
 21. (a) N. Inamoto and S. Matsuda, *Chem. Lett.*, 1982, 1003; (b) N. Inamoto and S. Matsuda, *Chem. Lett.*, 1982, 1007.
 22. (a) S. Gryaznov and J.-K. Chen, *J. Am. Chem. Soc.*, 1994, **116**, 5876; (b) V. Tereshko, S. Gryaznov, and M. Egli, *J. Am. Chem. Soc.*, 1998, **120**, 269.
 23. (a) E. Diez, J. San Fabián, J. Guillème, C. Altona, and L. A. Donders, *Mol. Phys.*, 1989, **68**, 49; (b) J. van Wijk, B. D. Huckriede, J. H. Ippel, and C. Altona, *Meth. Enzymol.*, 1992, **211**, 286.
 24. (a) C. A. G. Haasnoot, F. A. A. M. de Leeuw, and C. Altona, *Tetrahedron*, 1980, **36**, 2783. (b) C. Altona, *Recl. Trav. Chim. Pays-Bas*, 1982, **101**, 413.
 25. C. Altona, R. Francke, R. De Haan, J. H. Ippel, G. J. Daalmans, A. J. A. Westra Hoekzema, and J. van Wijk, *Magn. Reson. Chem.*, 1994, **32**, 670.